ELSEVIER

Journal of Biomechanics 32 (1999) 311–316

JOURNAL OF BIOMECHANICS

Technical Note

Quantitative anatomy of the lumbar musculature

Ian A.F. Stokes*, Mack Gardner-Morse

Department of Orthopaedics and Rehabilitation, University of Vermont, Burlington, VT 05405-0084, USA

Received in final form 22 September 1998

Abstract

This paper describes the anatomy of the musculature crossing the lumbar spine in a standardized form to provide data generally suitable for static biomechanical analyses of muscle and spinal forces. The muscular anatomy from several sources was quantified and transformed to the mean bony anatomy of four young healthy adults measured from standing stereo-radiographs. The origins, insertions and physiological cross-sectional area (PCSA) of 180 muscle slips which act on the lumbar spine are given relative to the bony anatomy defined by the locations of 12 thoracic and five lumbar vertebrae, and the sacrum, and the shape and positions of the 24 ribs. The broad oblique abdominal muscles are each represented by six vectors and an appropriate proportion of the total PCSA was assigned to each to represent the muscle biomechanics. © 1999 Elsevier Science Ltd. All rights reserved.

Keywords: Lumbar spine; Muscles; Anatomy; Tomography

1. Introduction

In static biomechanical analyses, whole muscles are usually represented as single vectors with a certain line of action and variable force magnitude. The line of action of a muscle may be considered to go directly from the origin to the insertion site, or it may be assumed to follow the centroids of the cross sections (e.g. CT images) of the muscle (Jenson and Davy, 1975) providing each section contains all of the fibers of the muscle (Koolstra et al., 1989).

Muscle force generating potential depends on the size, structure and length of the muscle. It is often considered to be proportional to the physiological cross-sectional area (PCSA) which is the volume divided by the pennated fiber length (Lieber, 1992). The muscle volume can be obtained from anatomical specimens, but cannot be calculated from a single cross-sectional image because the area varies along the muscle length (Lieber, 1992).

For the lumbar spine, the dorsal anatomy is very complex, with numerous slips of muscle which either connect to individual lumbar vertebrae, extend into the thorax, or attach inferiorly to the pelvis and/or sacrum, or the femora (psoas major). The abdominal muscles are layered curved sheets of muscle which have very long and curved attachments, and diverging fiber directions, making the centroid method unsuitable for these muscles. Different regions of the abdominals can be activated separately (Mirka et al., 1997). Faced with this complexity, many biomechanical representations of lumbar spinal musculature and associated static analyses have used a single cross section (typically at L3-L4) and have grouped the numerous muscle slips crossing this section into a simplified set of muscles. Each group is then considered to exert a single force at a specified angle to the cross-sectional plane. This approach ignores the actions of individual fascicles of the muscle groups, and also considers the action of each muscle only at the analyzed cross section, and not at other anatomical levels which it crosses. Furthermore, there is a wide reported range of directions for the muscle lines of action in the trunk (Han et al., 1992; Hughes et al., 1995; McGill, 1992, 1996) to which the calculated spinal and muscle forces are sensitive (Nussbaum et al., 1995).

The purpose of this paper is to combine data from available sources to quantify the anatomy of all muscles crossing the lumbar spine in a form generally suitable for static analyses of muscle forces and spinal forces. This requires definition of each muscle slip's attachment points (giving its line of action relative to all vertebrae),

* Corresponding author. Tel.: 802 656 2250; fax: 802 656 4247; e-mail: stokes@med.uvm.edu

PII: S0021-9290(98)00164-X

and its force generating capacity. The oblique abdominal muscles were represented by broad curved sheets of muscle divided into a set of six component parts, each represented by a single vector with individualized activation. The geometry was assumed to be symmetrical about the mid-sagittal plane.

2. Methods

A global coordinate system based on ISO 2631 was established with the origin at the center of the body of the first sacral vertebra, the X-axis forward, the Y-axis to the left and the Z-axis superior, with the subject standing in a relaxed upright position. For each vertebra, a local x, y, z coordinate system was defined as given in Stokes (1994).

The bony anatomy was obtained from reconstructions of the thoracic and lumbar spines and ribcages using standing stereo-radiographs of four young healthy adults (three males and one female, 25–36 yr-old, 45–82 kg, 1.65–1.8 m tall) obtained from a previous study (Dansereau and Stokes, 1988). The four spinal reconstructions were represented by the coordinates of the centers of each vertebra. These coordinates were normalized to the mean length of the spines, then averaged over the four subjects and the spine was made symmetrical about the sagittal plane by setting the Y-coordinates to zero. For the ribs, the average X, Z and absolute Y-values of 13 equally spaced points along each rib were obtained by spline fitting to give symmetrical 3-D coordinates defining the centers of the midlines of each of the 24 ribs in the global coordinate system.

Coordinates of the muscle origins and insertions were scaled, translated and rotated to fit the skeletal geometry, using the lumbar spinal vertebrae as a reference. Sagittal plane symmetry was assumed. To transform coordinates to the skeletal coordinate system, two landmarks common to both the skeletal and muscle data were first selected. The landmarks were the S1 vertebra center (the origin of axes) and the center of another vertebra, either T12 or L1. Muscle coordinates were then displaced, scaled and rotated in order to overlay vectors joining the two landmarks.

2.1. Abdominal muscles

The geometry of the abdominal muscles (rectus abdominis, and external and internal oblique muscles) was obtained from the datasets of the Visible Human Project™ (National Library of Medicine, Bethesda, MD), using transverse sections of the female (59 yr-old, 1.66 m tall) and male (38 yr-old, 1.8 m tall, 90 kg).

We omitted the transversus muscle because it is the smallest of the abdominal muscles, it does not have an anterior attachment to the skeleton, and its line of action is very curved. Dissections of two cadavers were examined to document the fiber directions of the oblique muscles. Transverse section photographic images from the Visible Human Project™ at 25 mm Z-direction intervals of the abdomen were examined for a total of 13 sections in the female and 12 sections in the male. For each muscle section, about 100 points on the outline of each section were digitized and converted to polar coordinates with the local origin arbitrarily at the vertebral center. The section was then divided into an internal and an external surface, with the boundary between them defined by the maximum and minimum value of angular polar coordinates of points on the outline. Thirteen points on each muscle inner and outer surface were then interpolated by first fitting a cubic spline function to the digitized polar coordinates. The right and left sides were averaged, as was done for the ribs (see above), and scaled and rotated to the coordinate system of the reference skeleton (see Fig. 1).

The resulting volumetric reconstructions were expressed as a single equivalent line of action for each side of the rectus abdominis, and six lines of action representing six components parts of each of the internal and external oblique muscles. For rectus abdominis, the vector for each side was determined by linear regression of the x and z, and the y and z values of the centroids of the muscle area of each of the cross sections. The regression line showed that the muscle path was almost straight, and passed within 10 mm of the centroids at the extremes of the muscle path. The centroid method is appropriate here, because the rectus abdominis cross sections included all of the muscle fibers, and because it was considered that for most of the path the sections were of uniform composition (contractile tissue).

For the obliques, the six vectors were drawn by a subjective, empirical method with a best compromise matching three conditions: (1) terminate on pelvis or ribs (when appropriate), be oriented in directions corresponding to predominant fiber directions photographed in dissections of cadavers, and (3) be contained within the volume identified by the outlines of the serial sections (see Figs. 1 and 2).

In order to divide the total PCSA between the six component vectors, the points of intersection of the six vectors with each image section were first located. Then normals to the line passing through these points were calculated, and their intersections with the inside and outside outlines of the corresponding muscle were determined. These normal lines subdivided the total area into a set of partial areas, one for each vector (see Fig. 2). The volume associated with each vector was calculated as the sum of its partial areas multiplied by the separation between cross sections (nominally 25 mm). The effective PCSA of each of the six muscle components was obtained as its partial volume divided by the length of the respective vector. Lastly, the muscle attachment points and PCSA for the female and male were averaged.

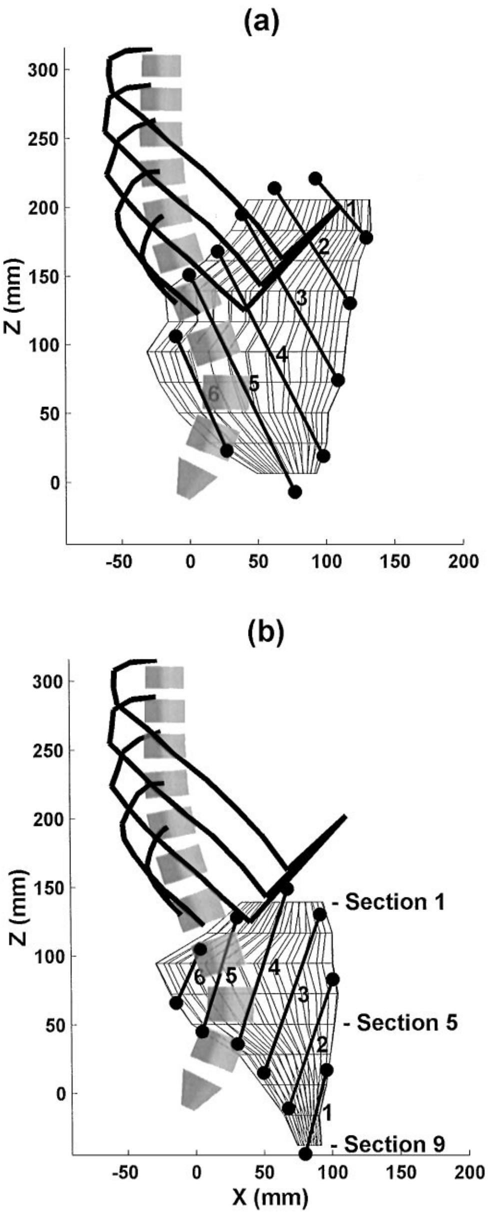

Fig. 1. Lateral views of the six muscle slips of the male Visible Human™ external oblique (a) and internal oblique (b) and the 8th–12th ribs and vertebrae T8 through S1. The volumes of the obliques are shown as meshes with lines connecting adjacent points in the horizontal planes and between the sections. Sections 1, 5 and 9 of internal oblique are labeled in (b).

2.2. Quadratus lumborum and psoas

The quadratus lumborum was represented by five fascicles on each side of the spine, joining the center of the 12th rib and the first four lumbar vertebrae to the ilium. Serial CT sectional data published by Han et al. (1992) give the total cross-sectional area of these muscles at each anatomical level (averaged for 10 subjects 24–70 yr-old, 44.9–72 kg, 1.44–1.74 m tall). The level-by-level differences of this area were considered to be the PCSA of the fascicle arising at each level. The point of attachment of quadratus lumborum to the iliac crest was found from the Visible Human Project™ images and the right and left sides of both the female and male images were averaged.

Each side of the psoas major was represented by eleven fascicles arising from the vertebral bodies, transverse processes and intervertebral discs. Their points of attachment relative to each vertebra and their PCSA were obtained from data on three embalmed cadavers published by Bogduk et al. (1992b). Distally, they have a common tendon which passes over the ilium, and this point was considered to be the effective distal attachment. Its position was averaged from the points measured from the Visible Human Project™ images. Since certain slips (fascicles) were not present in all of the muscle specimens, the corresponding PCSA values were weighted in proportion to their prevalence as found by Bogduk et al. (1992b).

2.3. Dorsal muscles

The dorsal muscles were considered to consist of numerous fascicles of three groups of muscles: longissimus, iliocostalis, and multifidus. The PCSA of the individual slips and their attachment points relative to the local coordinates of the lumbar vertebrae and sacrum were obtained from Bogduk et al. (1992a) who published data for eight adult embalmed cadavers. The local coordinates of attachment points described by anatomical landmarks were measured directly, from stereo X-rays of anatomical specimens, and by using the thoracic vertebral morphology data of Panjabi et al. (1991). Coordinates of the attachment points in the local vertebral x, y, z coordinates were then transformed into the global X, Y, Z coordinate system.

An additional five muscle pairs beyond those specified by Bogduk et al. (1992a) were added to represent the thoracic multifidi that attach in the lumbar region, and they were assigned PCSAs of 40 mm^2 (the average for the lumbar multifidi). Three fascicles of thoracic multifidus originate on each thoracic spinous process and attach to the mammillary processes of lumbar vertebrae three, four and five levels caudal to the thoracic vertebrae (Bogduk, 1993, personal communication).

The rib and transverse process attachments of longissimus pars thoracis and iliocostalis pars thoracis were assigned to points on the ribs of the skeleton based on MacIntosh and Bogduk (1991). The rib attachments were considered to be 3 mm posterior and 4 mm below the measured rib midlines.

Because of the convex curvature of the thoracic spine and ribcage, 30 fascicles (15 pairs) with attachments high in the thoracic spine could not take a straight line path from origin to insertion without passing inside the ribs.

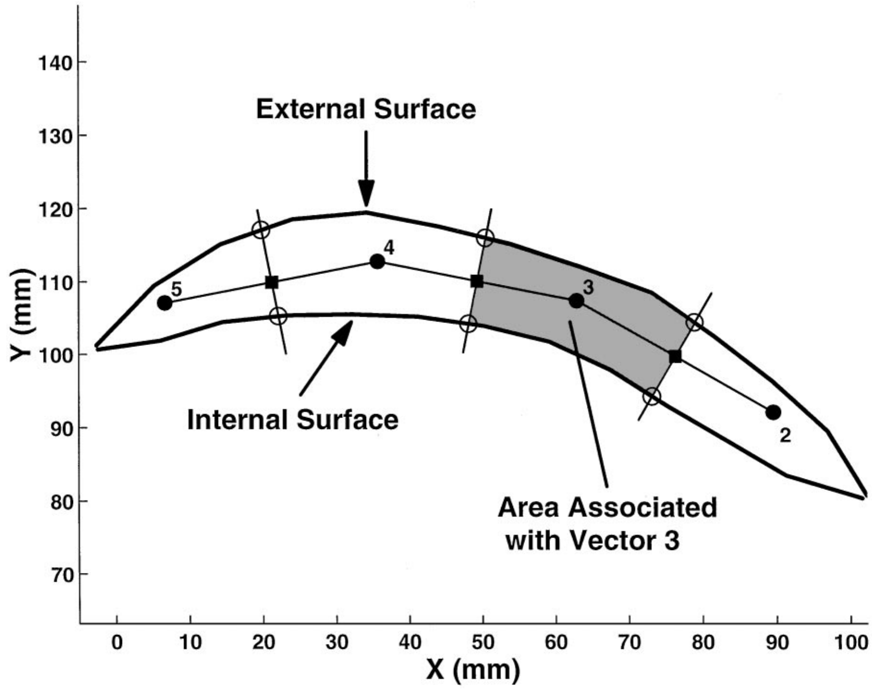

Fig. 2. A section of the male Visible Human™ internal oblique showing the method of dividing the area of the section between the muscle component vectors. The intersections of muscle components vectors 2–5 with this section (components 1 and 6 did not pass through this section) are numbered (●). These points were connected by lines, and perpendiculars were constructed at their midpoints (■). The intersections (○) between the perpendiculars and the original section outline (internal and external surfaces of the muscle) divides the section into partial areas for each muscle component vector (shaded area for vector 3).

For these muscles, the muscle lines of action were projected onto the surface overlaying the posterior aspects of the ribs and the transverse processes to determine a set of intermediate points. The chosen intermediate point was the one whose line joining it to the inferior attachment point made the greatest angle with the line joining the origin to the insertion.

3. Results

The 3-D coordinates of the vertebrae centers T1–S1 are given in Table 1. The total volumes of the abdominal muscles obtained from the two sources are presented in Table 2. The relative volumes of the external oblique, internal oblique and transversus muscles were 51, 28 and 21%, respectively (Table 2), and these relative proportions are similar in both sources of data.

Lateral and A-P views of the spine, ribcage and left side of the symmetric muscle geometry are shown in Fig. 3 (available on the Journal of Biomechanics web site www.elsevier.nl/locate/jbiomech). The abdominal muscle anatomy is given in Table 3 for the left side (the right side is symmetric). Similarly, the dorsal muscle anatomy is given in Table 4 available on the web site www.elsevier.nl/locate/jbiomech. For each of the dorsal muscles which wrapped over the ribcage Table 4 gives two origins corresponding to the actual attachment to the rib cage and the point where it wraps around the ribcage.

Table 1
Positions of vertebral body centers (standing posture) in global coordinates. The mean of four subjects is given, with the standard deviation in parentheses

Vertebra name	X (mm)	Y (mm)	Z (mm)
T1	−3.1 (21.2)	0.0	454.9 (0.54)
T2	−14.4 (17.2)	0.0	437.3 (0.93)
T3	−20.8 (13.4)	0.0	418.0 (1.38)
T4	−23.0 (14.0)	0.0	397.2 (1.24)
T5	−22.8 (13.5)	0.0	375.3 (1.81)
T6	−21.5 (16.1)	0.0	351.5 (1.54)
T7	−20.4 (15.4)	0.0	326.8 (2.37)
T8	−20.0 (15.4)	0.0	302.5 (2.13)
T9	−20.2 (15.9)	0.0	278.2 (2.35)
T10	−20.4 (17.0)	0.0	252.8 (2.16)
T11	−19.5 (16.9)	0.0	225.1 (2.56)
T12	−15.8 (14.4)	0.0	196.0 (2.39)
L1	−8.4 (8.3)	0.0	166.3 (2.67)
L2	3.6 (12.6)	0.0	133.9 (2.01)
L3	17.4 (13.0)	0.0	100.6 (1.89)
L4	26.2 (13.1)	0.0	64.8 (1.80)
L5	16.2 (4.2)	0.0	31.7 (1.02)
S1	0.0	0.0	0.0

4. Discussion

This study combines data for the lumbar spinal muscle attachments and PCSAs from several sources. Since the muscle geometry is referred to vertebrae, it is in a form which can be readily transformed geometrically to fit a specified spinal shape (e.g. Stokes, 1997), assuming that the muscles are rigidly attached to the vertebrae, and assuming that they follow straight lines from origins to insertions (i.e. there are no intermediate muscle wrap points).

The values reported here are referred to average-sized adults in the standing posture. However, the numbers of subjects examined was small, and the data were assembled from differing sources (radiographs of four living subjects, published anatomical data, examinations of two cadavers and the two individuals documented by the photographic images of the cryosections of the Visible Human Project™). The latter gave a clear distinction between the muscle layers of the abdominal wall (except at the upper and lower extremes) which was not possible in MRI and CT images that we examined.

Linear geometrical scaling was used to combine data from different individuals since Wood et al. (1996) have shown that muscle area does not correlate well with trunk area, apparently because of variable amounts of fat tissue. Muscle volumes would be the most sensitive to scaling (scale cubed effect) and more so than PCSAs (scale squared effect) and the attachments (linear effect).

In comparison with previously published data for the abdominal muscles, we found each side of rectus abdominis to have PCSA of 567 mm^2, compared to area values in the range 360–850 mm^2 from Takashima et al. (1979); Reid and Costigan (1985), Han et al. (1992) and McGill (1996). For external oblique we obtained 1575 mm^2 as the total of the six-component muscle vectors, compared to 960 mm^2 for the sum of three parts in Takashima et al. (1979) and 1600 mm^2 from McGill (1996), who summed two parts. For internal oblique we obtained 1345 mm^2 for the total of the six muscle components, compared to 1090 mm^2 for the sum of three parts in Takashima et al. (1979) and 1950 mm^2 for the total of two muscle components in McGill (1996). Therefore, the results given here are within the previously reported range.

Van der Helm and Veenbaas (1991) showed that at least six vectors are required to represent the forces and moments produced by muscles with broad curved muscle attachments, so this number of muscle components was used to represent the oblique abdominals. The internal

Table 2
Volumes of the Visible Human™ abdominal muscles using 8 point integration

Muscle name	Female (mm^3)	Male (mm^3)
External Oblique	171 030	220 053
Internal Oblique	93 407	138 794
Transversus	78 616	96 512
Rectus Abdominus	152 095	161 878

Table 3
Abdominal muscle names, PCSAs, and coordinates and anatomical locations of muscle attachments. Values in parentheses are the differences between values from the male and female subject. (Data for left side of subject – for the right side, negate the Y value)

Muscle name	PCSA (mm^2)	Origin			Upper attachment	Insertion			Lower attachment
		X (mm)	Y (mm)	Z (mm)		X (mm)	Y (mm)	Z (mm)	
External Oblique									
Ext1	195.7	78.0 (30)	117.0 (0)	246.5 (51)	Ribs	118.0 (24)	79.5 (9)	189.0 (22)	S/P
Ext2	231.7	47.5 (31)	137.0 (2)	240.5 (53)	Ribs	112.5 (11)	100.5 (19)	137.0 (14)	S/P
Ext3	243.2	33.5 (11)	142.0 (2)	204.5 (19)	Ribs	115.0 (12)	110.5 (27)	65.0 (18)	S/P
Ext4	234.4	19.5 (3)	141.5 (3)	171.5 (7)	Ribs	102.0 (8)	116.0 (46)	20.0 (2)	S/P
Ext5	273.0	−1.5 (3)	134.5 (3)	155.5 (9)	Ribs	73.5 (7)	134.0 (40)	9.0 (32)	S/P
Ext6	397.4	−14.0 (8)	122.0 (6)	115.0 (18)	Ribs	25.5 (3)	137.5 (21)	36.5 (27)	S/P
Internal oblique									
Int1	185.3	109.5 (27)	91.0 (38)	20.5 (7)	Ribs	98.0 (36)	96.5 (23)	−30.5 (27)	S/P
Int2	224.3	111.0 (20)	98.5 (21)	90.0 (14)	Ribs	84.0 (32)	114.0 (28)	−7.0 (8)	S/P
Int3	226.0	99.0 (14)	113.0 (14)	129.0 (2)	Ribs	66.0 (32)	124.5 (33)	18.5 (7)	S/P
Int4	267.6	81.5 (27)	114.5 (7)	164.0 (30)	Ribs	44.0 (26)	132.0 (40)	40.0 (8)	S/P
Int5	235.0	41.5 (21)	134.5 (25)	123.5 (9)	Ribs	15.5 (21)	122.0 (32)	48.5 (7)	S/P
Int6	207.2	14.0 (20)	129.5 (31)	112.0 (14)	Ribs	−7.5 (13)	112.0 (34)	66.5 (1)	S/P
Rectus Abdominus									
RecAb	567.0	130.0 (33)	47.3 (9)	259.7 (54)	Ribs	128.7 (45)	35.4 (1)	−38.0 (1)	S/P

X = forwards; Y = left; Z = up in a global coordinate system for a standing subject.
Ribs = Ribcage (directly or via fascia). S/P = Sacrum/Pelvis (directly or via fascia).

oblique muscles were well represented by straight lines, as evidenced by the six lines used here fitting well within the reconstructed muscle volume. Since straight muscles cannot generate intra-abdominal pressure, this implies that other muscles (presumably diaphragm and transversi) would be required for intra-abdominal pressurization, although the obliques may become more curved under the influence of abdominal pressurization.

Acknowledgements

This work was supported by NIH award R01 AR 44119. The authors thank Drs. Nikolai Bogduk and Mark Pearcy for generous assistance and for access to original data, Drs. Mary Moffroid and Sharon Henry and Mr. Bruce Fonda for their helpful discussions of anatomy and assistance with the cadavers, and the digitizing and programming assistance of Sarah Young and Andy Crighton.

References

Bogduk, N., 1993. Personal communication, 6 January 1993. The University of Newcastle, Newcastle, NSW 2308, Australia.

Bogduk, N., Macintosh, J.E., Pearcy, M.J., 1992a. A universal model of the lumbar back muscles in the upright position. Spine 17, 897–913.

Bogduk, N., Pearcy, M., Hadfield, G., 1992b. Anatomy and biomechanics of psoas major. Clinical Biomechanics 7, 109–119.

Dansereau, J., Stokes, I.A.F., 1988. Measurements of the three-dimensional shape of the rib cage. Journal of Biomechanics 21, 893–901.

Han, J.S., Ahn, J.Y., Goel, V.K., Takeushi, R., McGowan, D., 1992. CT-based geometric data of human spine musculature. Part 1. Japanese patients with chronic low back pain. Journal of Spinal Disorders 5, 448–458.

Hughes, R.E., Bean, J.C., Chaffin, D.B., 1995. Evaluating the effect of co-contraction in optimization models. Journal of Biomechanics 28, 875–878.

Jenson, R.H., Davy, D.T., 1975. An investigation of muscle lines of action about the hip: A centroid line approach versus the straight line approach. Journal of Biomechanics 8, 103–110.

Koolstra, J.H., van Eijden, T.M., Weijs, W.A., 1989. An iterative procedure to estimate muscle lines of action in vivo. Journal of Biomechanics 22(8–9), 911–920.

Lieber, R.L., 1992. Skeletal Muscle Structure and Function: Implications for Rehabilitation and Sports Medicine. Williams and Wilkins, Baltimore.

MacIntosh, J.E., Bogduk, N., 1991. The attachments of the lumbar erector spinae. Spine 16, 783–792.

McGill, S.M., 1992. A myoelectrically based dynamic three-dimensional model to predict loads on lumbar spine tissues during lateral bending. Journal of Biomechanics 25, 395–414.

McGill, S.M., 1996. A revised anatomical model of the abdominal musculature for torso flexion efforts. Journal of Biomechanics 29, 973–977.

Mirka, G., Kelaher, D., Baker A., Harrison A., Davis, J., 1997. Selective activation of the external oblique musculature during axial torque production. Clinical Biomechanics 12, 172–180.

Nussbaum, M.A., Chaffin, D.B., Rechtien, C.J., 1995. Muscle lines-of-action affect predicted forces in optimization-based spine muscle modeling. Journal of Biomechanics 28, 401–409.

Panjabi, M.M., Takata, K., Goel, V., Federico, D., Oxland, T., Duranceau, J., Krag, M., 1991. Thoracic human vertebrae. Quantitative three-dimensional anatomy. Spine 16, 888–901.

Reid, J.G., Costigan, P.A., 1985. Geometry of adult rectus abdominis and erector spinae muscles. Journal of Orthopaedics and Sports physical Therapy 6, 278–280.

Stokes, I.A.F., 1994. Three-dimensional terminology of spinal deformity. A report presented to the Scoliosis Research Society by The Scoliosis Research Society Working Group on 3-D Terminology of Spinal Deformity. Spine 19, 236–248.

Stokes, I.A.F., 1997. Analysis of symmetry of vertebral body loading consequent to lateral spinal curvature. Spine 22(21), 2495–2503.

Takashima, S.T., Singh, S.P., Haderspeck, K.A., Schultz, A.B., 1979. A model for semi-quantitative studies of muscle actions. Journal of Biomechanics 12, 929–939.

Van der Helm, F.C.T., Veenbaas R., 1991. Modelling the mechanical effect of muscles with large attachment sites: application to the shoulder mechanism. Journal of Biomechanics 24, 1151–1163.

Wood, S., Pearsall, D.J., Ross, R., Reid, J.G., 1996. Trunk muscle parameters determined from MRI for lean to obese males. Clinical Biomechanics 11, 139–144.